Supplementary Information for:

Copper Binding to the N-Terminally Acetylated, Naturally Occurring Form of Alpha-Synuclein Induces Local Helical Folding

Marco C. Miotto,[†,‡] Ariel A. Valiente-Gabioud,[†,‡] Giulia Rossetti,[§] Markus Zweckstetter,[∥,⊥,#] Paolo Carloni,[§] Philipp Selenko,[▽] Christian Griesinger,[∥] Andres Binolfi,[,†,‡,▽] and Claudio O. Fernández[*,†,‡]*

[†]Max Planck Laboratory for Structural Biology, Chemistry and Molecular Biophysics of Rosario and [‡]Instituto de Investigaciones para el Descubrimiento de Fármacos de Rosario (IIDEFAR/CONICET-UNR), Universidad Nacional de Rosario, 27 de Febrero 210 bis, S2002LRK Rosario, Argentina

[§]Computational Biophysics, German Research School for Simulation Sciences and Computational Biomedicine, Institute for Advanced Simulations IAS-5, Forschungszentrum Jülich, D-52425 Jülich, Germany

[∥]Department of NMR-based Structural Biology, Max Planck Institute for Biophysical Chemistry, Am Fassberg 11, D-37077, Göttingen, Germany

[⊥]Deutsches Zentrum für Neurodegenerative Erkrankungen, 37077 Göttingen, Germany

[#]Center for the Molecular Physiology of the Brain, University Medical Center, 37077 Göttingen, Germany

[▽]Department of NMR-assisted Structural Biology, In-cell NMR, Leibniz Institute of Molecular Pharmacology, Robert-Roessle-Strasse 10, 13125 Berlin, Germany

Supplementary methods

Protein and reagents. ^{15}N and ^{15}N-^{13}C isotopically enriched AS and N-terminally acetylated AS (AcAS) were obtained by transfecting *E. coli* BL21 cells with a plasmid harboring the wild type AS gene (for AS) together with a second plasmid encoding the components of yeast NatB acetylase complex (for AcAS).[1] Plasmids carried different antibiotic resistance, namely Ampicillin and Chloramphenicol, to select the doubly transformed *E. coli* colonies. Purification was carried out as previously reported,[2] with the exception that both antibiotics were included in the growth flasks to avoid plasmid purge during growth and expression. The final purity of the AcAS samples was determined by SDS-PAGE. No residual amounts of NatB protein were detected in the AcAS samples. Acetylation was complete in all sample preparations as attested by ^{1}H-^{15}N heteronuclear NMR spectroscopy. Copper chloride, L-ascorbic acid, MES buffer and D_2O were purchased from Merck or Sigma. The chemicals 4,4-Dimethyl-4-silapentane-1-sulfonic acid (DSS), ^{15}N NH_4Cl and U-^{13}C glucose were purchased from Cambridge Isotope Laboratories or Sigma. Purified protein samples were dissolved in 20 mM MES buffer supplemented with 100 mM NaCl at pH 6.5 (Buffer A) or in 20 mM MOPS buffer supplemented with 100 mN NaCl at pH 7.4 (Buffer B). Protein concentrations were determined spectrophotometrically by measuring absorption at 274 nm and using an epsilon value of 5600 $M^{-1}cm^{-1}$.

NMR experiments. NMR spectra were recorded on Bruker 600 MHz Avance II and 750 MHz Avance spectrometers, equipped with cryogenically cooled triple resonance ^{1}H(^{13}C/^{15}N) TCI probes. The 2D experiments ^{1}H-^{15}N SOFAST-HMQC, ^{1}H-^{13}C HSQC, ^{15}N R_1 and ^{15}N R_2 relaxation rates, ^{1}H-^{15}N heteronuclear NOE, and the 3D experiments ^{15}N-edited TOCSY and NOESY-HSQC, HNHA, HNCO and HNCACB were all recorded at 15^{o}C using protein samples dissolved in buffer A. Direct ^{13}C-detection, ^{13}CO-^{15}N HflipCON and ^{13}CO-

$^{13}C\alpha$ H-flipCαCO experiments were recorded at 37^{o}C using protein samples dissolved in buffer B. NMR parameters used in each experiment are described next. ^{1}H-^{15}N SOFAST-HMQC[3]: 16 scans, 1024 complex points (16 ppm in the ^{1}H dimension) and 256 complex points (26 ppm in the ^{15}N dimension). ^{13}CO-^{15}N H-flipCON and ^{13}CO-$^{13}C\alpha$H-flipCαCO experiments[4] were acquired with 256 and 128 scans, respectively, using 1024 complex points and a sweep width of 16 ppm for the direct ^{13}CO dimension. A total of 128 increments (resulting from 256 IPAP increments) and sweep widths of 26 ppm for the ^{15}N and 34 ppm for the $^{13}C\alpha$ dimensions were used. ^{15}N R_1 and R_2 relaxation rates, and ^{1}H-^{15}N NOE data were acquired at 750 MHz external field using modern versions of pulse sequences based on those described by Farrow *et al*.[5] Experiments were recorded with 1024 complex points for a sweep width of 16 ppm for the ^{1}H dimension and 256 complex points in the ^{15}N dimension for a sweep width of 26 ppm. R_1 and R_2 relaxation rates were obtained by recording the experiments with different T1 and T2 delays.[5] Resonance heights at each spectra were fit to a two parameter exponential decay function where the independent variable was the relaxation delay. Steady-state ^{1}H-^{15}N NOE (hetNOEs) values were obtained from the ratio of peak heights in paired spectra collected with and without an initial 4 s period of proton saturation during the recycling delay. 3D experiments were recorded using Bruker standard pulse sequences with the following parameters. HNCACB: complex points: 1024 (^{1}H), 64 (^{15}N), 110 (^{13}C); spectral width (ppm), 16 (^{1}H), 26 (^{15}N), 66 (^{13}C); number of scans, 16. HNCO: complex points: 1024 (^{1}H), 64 (^{15}N), 96 (^{13}C); spectral width (ppm), 16 (^{1}H), 26 (^{15}N), 16 (^{13}C); number of scans, 4. HNHA: complex points: 1024 (^{1}H), 80 (^{15}N), 144 (^{1}H); spectral width (ppm), 16 (^{1}H), 26 (^{15}N), 10 (^{1}H); number of scans, 16. ^{15}N-edited TOCSY-HSQC: complex points: 1024 (^{1}H), 80 (^{15}N), 128 (^{1}H); spectral width (ppm): 16 (^{1}H), 26 (^{15}N), 14 (^{1}H); number of scans, 4; TOCSY spin-lock, 9.2 KHz and TOCSY mixing time, 200 ms. ^{15}N-edited NOESY-HSQC: complex points: 1024 (^{1}H), 80 (^{15}N), 128 (^{1}H); spectral width (ppm): 16 (^{1}H), 26 (^{15}N), 14 (^{1}H); number of scans, 8; NOESY mixing time, 100 ms.

Sequence-specific assignments for the backbone of free and Cu(I)-bound AcAS and AS were obtained using the above mentioned triple resonance experiments. Secondary chemical shift values were calculated as the difference between the measured Cα and Cβ chemical shifts and the empirical random coil values reported by the Wishart lab.[6] The deviation of the observed chemical shifts from consensus random coil values is indicative of secondary structure. Positive or negative deviations in Cα shifts are indicative of α or β secondary structure, respectively; for Cβ the opposite trend is valid. DSS was used for chemical shift referencing. Neighbor corrected secondary structure propensity (SSP) scores were calculated using Cα and Cβ chemical shifts as input as previously described.[7,8] A 5 residues window average was used in both cases. Positive SSP values ranging from 0 to 1 and negative values from 0 to -1 represent the propensities of α and β structures, respectively. Three-bond HN-Hα coupling constants ($^3J_{HN\text{-}H\alpha}$) were obtained from the ratio between the intensities of the diagonal peaks and cross-peaks in the HNHA[9] experiment, as previously described.[10,11] Three-bond HN-Hα coupling constants ($^3J_{HN\text{-}H\alpha}$) are sensitive to the torsion angle ϕ populated by each residue in the protein sequence and thus report on secondary structure content. This coupling falls in the range 3.0–6.0 Hz for an α-helix and 8.0–11.0 Hz for a β-sheet structure. For a random-coil, a weighted average of these values is observed, that typically ranges between 6.0 and 8.0 Hz for most residues.[12,13] ^{1}H-^{1}H NOE intensity ratios between crosspeaks $d_{\alpha N}(i,i)$ and $(i–1,i)$ are very sensitive to the value of the ψ angle of residue i – 1 and report on secondary structure content of proteins and peptides.[14] NOE intensity ratio profiles were obtained as previously described[14] from ^{15}N-edited NOESY-HSQC experiments. Only unambiguously assigned, well resolved peaks were included in the analysis. For the intensity (I/I_0) profiles, ^{1}H–^{15}N SOFAST-HMQC protein amide cross-peaks affected during Cu(II) titration were identified by comparing their intensities (I) with those of the same cross-peaks (I_0) in the data set of samples lacking metal ions. The I/I_0 ratios obtained for well-

resolved cross-peaks were plotted as a function of the protein sequence to obtain the profiles. Mean weighted chemical shifts (^{1}H-^{15}N and ^{13}CO-^{15}N MWCS) were calculated as $[(\Delta\delta^{1}H)^2 + (\Delta\delta^{15}N/10)^2]^{1/2}$ and $[(\Delta\delta^{13}CO/4)^2 + (\Delta\delta^{15}N/10)^2]^{1/2}$.[15] Acquisition and processing of NMR spectra were performed using TOPSPIN 3.1 (Bruker Biospin). 2D spectra analysis and visualization were performed with Sparky.[16] For the sequence specific backbone assignments and $^{3}J_{HN\text{-}H\alpha}$ couplings calculation, the software CARA was used.[17] R_1 and R_2 relaxation data fitting was performed using Sparky routines.

Generation of Cu(I) complexes. To generate the Cu(I) complexes with AcAS the Cu(II) complexes were first prepared and then reduced with an excess of ascorbate. In all cases, the concentration of ascorbate used was 200:1 relative to the amount of added Cu(II).[18-20] After pH adjustment, samples were treated with a flow of N_2 during 5 minutes to generate a N_2 atmosphere. Spectra were recorded at 15°C on a Jasco V-550 spectrophotometer.

AcAS-Cu(I) complex affinities. The affinity features of Cu(I) binding to AcAS were determined from ^{1}H-^{15}N SOFAST-HMQC experiments using 50 µM protein samples recorded at increasing concentrations of the metal ion. Changes in ^{1}H-^{15}N MWCS values of amide resonances of AcMet-1, Asp-2, Val-3, Phe-4, Met-5, Lys-6, Gly-7 and Leu-8 (Site 1), His-50, Gly-51 and Val-52 (Site 2) and Asp-119, Asp-121, Asn-122 and Ala-124 (Site 3) of AcAS were used to simultaneously fit the data to a model incorporating complexes of Cu(I) in three classes of independent, non-interactive binding sites using the program DynaFit,[21] as previously reported for non-acetylated AS.[19]

Supplementary Figure 1

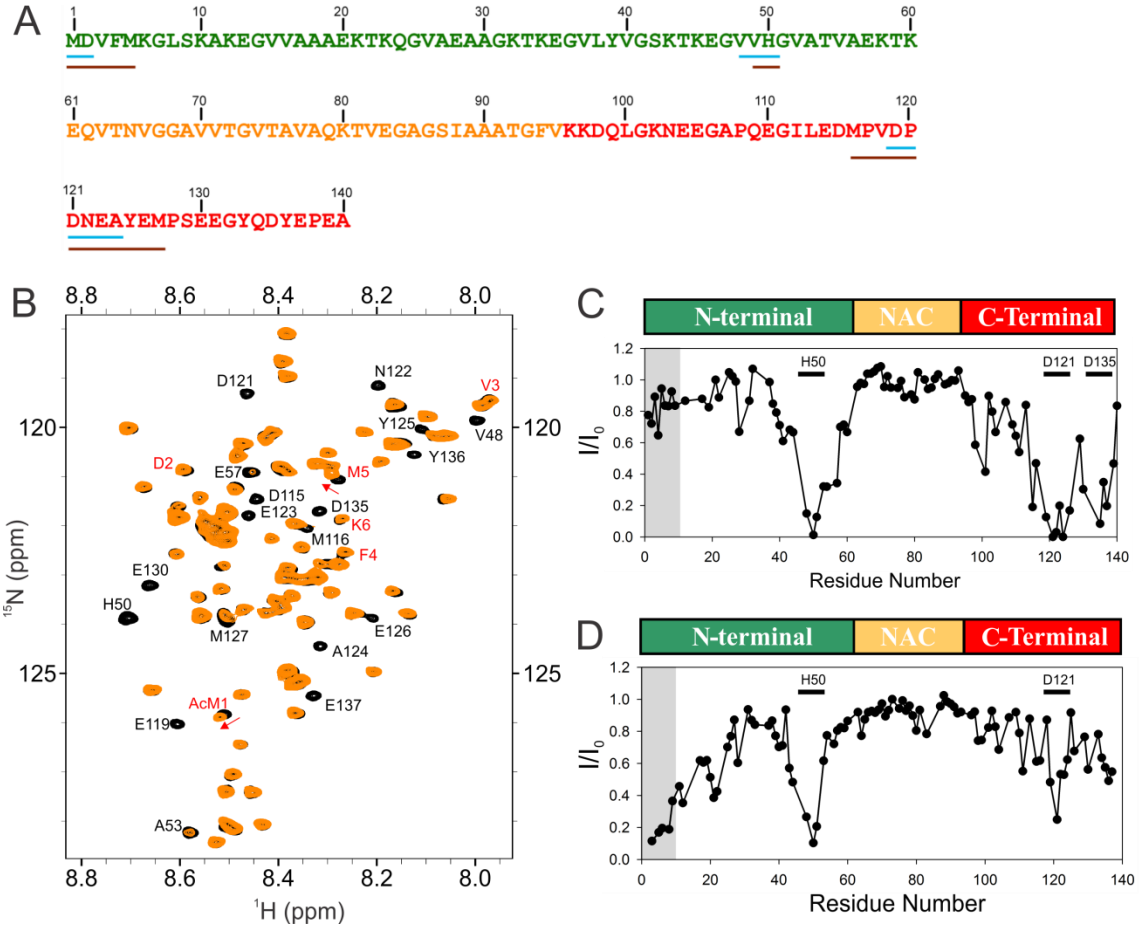

Supp. Fig. 1. NMR analysis of Cu(II) binding to AcAS. (A) Primary sequence of AS. Green, orange and red depict the N-terminal, NAC and C-terminal regions, respectively. Cyan and brown lines identify the Cu(II) and Cu(I) binding motifs previously identified in AS.[22] (B) Overlaid ^{1}H-^{15}N SOFAST HMQC spectra of AcAS in the absence (black) and presence (orange) of 0.6 equiv. of added Cu(II). Amino acid residues broadened significantly or beyond detection are identified in black. Residues labelled in red depict the sequence ^{1}AcMDVFMK^{6} in AcAS. (C, D) I/Io profiles of the backbone amide groups of 50 μM AcAS (C) and 50μM AS (D) in the presence of 0.5 equiv. of Cu(II). As shown in panel D, the strongest broadening effects due to Cu(II) binding to AS were centred on Met-1/Asp-2 (Site 1), His-50 (Site 2) and Asp-121 (Site 3).[22,23] Panel C reveals that N-terminal acetylation abolishes Cu(II) binding to site 1 in AcAS, whereas metal interaction with sites 2 and 3 remains unaffected. Gray boxes contain the first 10 residues of AS and AcAS sequence. Spectra were recorded at 15^{o}C using ^{15}N isotopically enriched AcAS or AS samples (50 μM) dissolved in buffer A.

Supplementary Figure 2

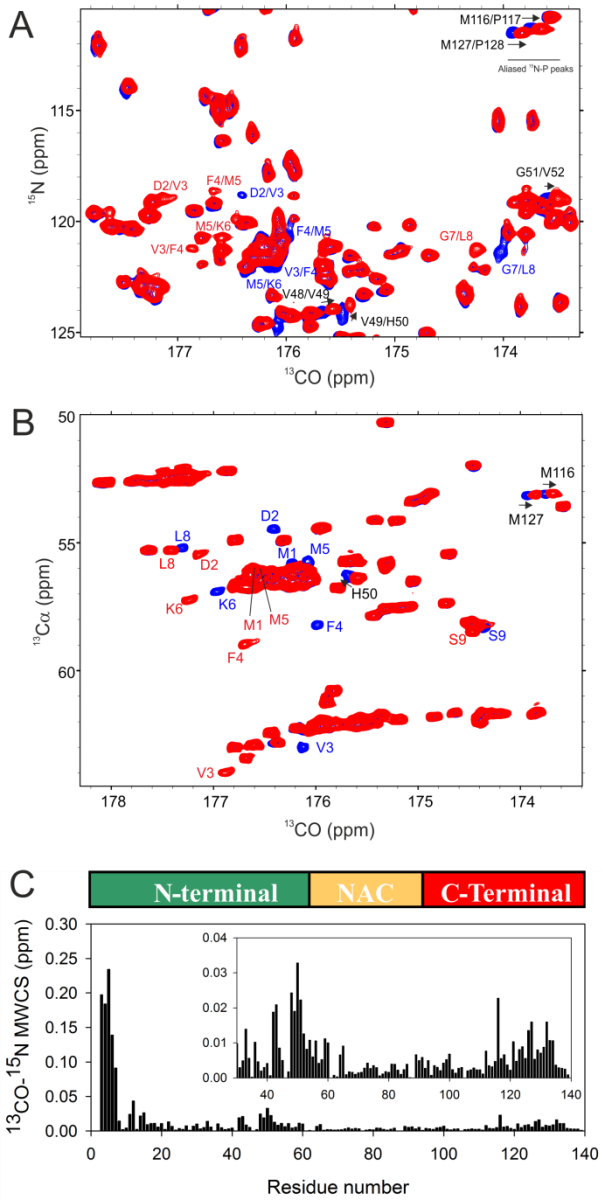

Supp. Fig. 2. NMR analysis of Cu(I) binding to AcAS at pH 7.4 and 37°C. (A, B) Overlaid ^{13}CO-^{15}N HflipCON (A) and ^{13}CO-^{13}Cα HflipCOCα (B) spectra of AcAS in the absence (blue) and presence (red) of 2 equiv. of Cu(I). Crosspeaks shifted significantly by the interaction with the metal ion are identified: free protein (blue) and metal-bound form (red). Black labels identify residues form sites with less pronounced chemical shifts perturbations. In panel A, correlations shown in the ^{13}CO-^{15}N HflipCON spectra correspond to the carbonyl of residue i and the amide nitrogen of residue i+1. In panel B, intraresidue Cα-CO correlations are shown. (C) Differences in the ^{13}CO-^{15}N mean weighted chemical shifts (^{13}CO-^{15}N MWCS) between free and Cu(I)-complexed AcAS at a molar ratio of 2:1. The inset shows an enlargement of the region corresponding to amino acids 30-140. Spectra were recorded using ^{15}N/^{13}C isotopically enriched AcAS samples (300 μM) dissolved in buffer B.

Supplementary Figure 3

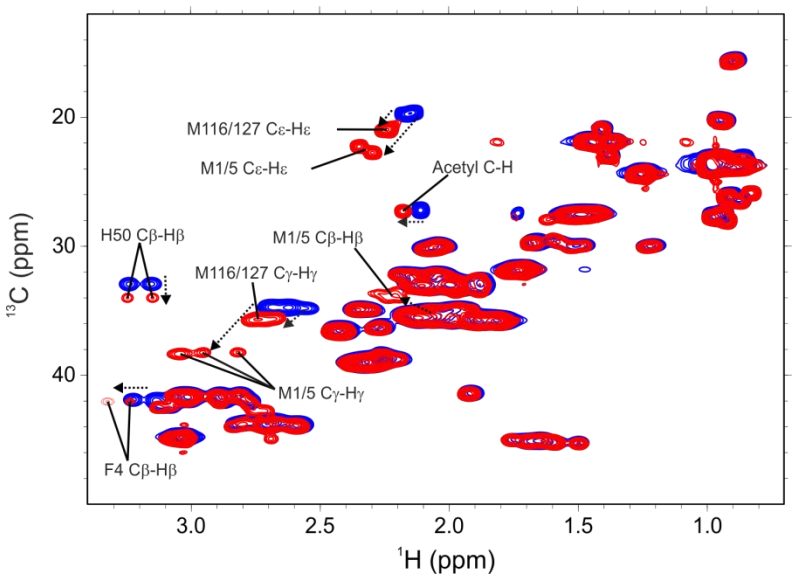

Supp. Fig. 3. Interaction between AcAS and Cu(I). ^{1}H-^{13}C HSQC of AcAS in the absence (blue) and presence of 2 equiv. of Cu(I) (red). The positions of crosspeaks experiencing chemical shifts upon Cu(I) binding are indicated. Spectra were recorded at 15^{o}C using ^{15}N/^{13}C isotopically enriched AcAS (300 μM) dissolved in buffer A.

Supplementary Figure 4

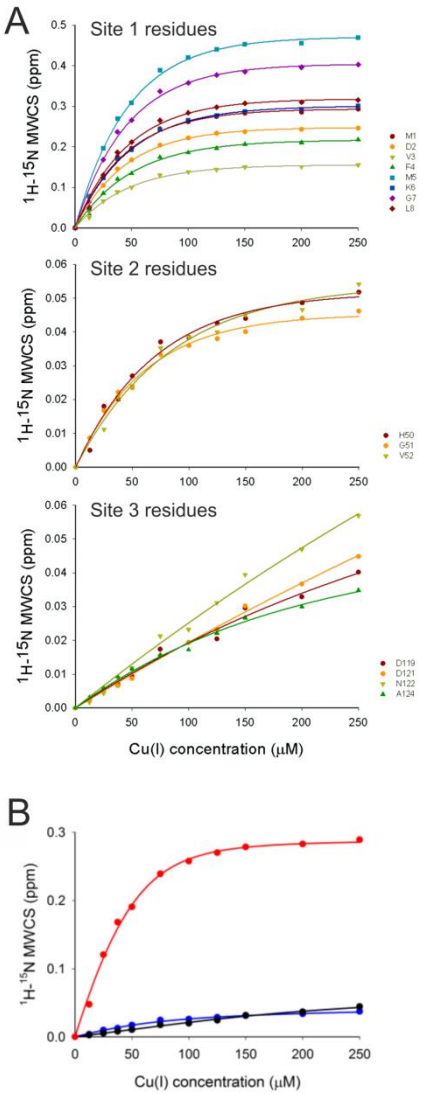

Supp. Fig. 4. Affinity features of Cu(I) binding to AcAS. (A) Binding curves of Cu(I) to AcAS, as monitored by changes in the mean weighted chemical shifts **(**^{1}H-^{15}N MWCS) of amide groups of amino acid residues involved in Cu(I) binding at each metal site. (B) Comparative mean binding curves of Cu(I) at the metal binding sites of AcAS: Site 1 (red), Site 2 (blue) and Site 3 (black). Curves represent the fit to the models described in the Supplementary Information. Experiments were performed at 15^{o}C using^{15}N isotopically enriched AcAS samples (50 μM) dissolved in buffer A.

Supplementary Figure 5

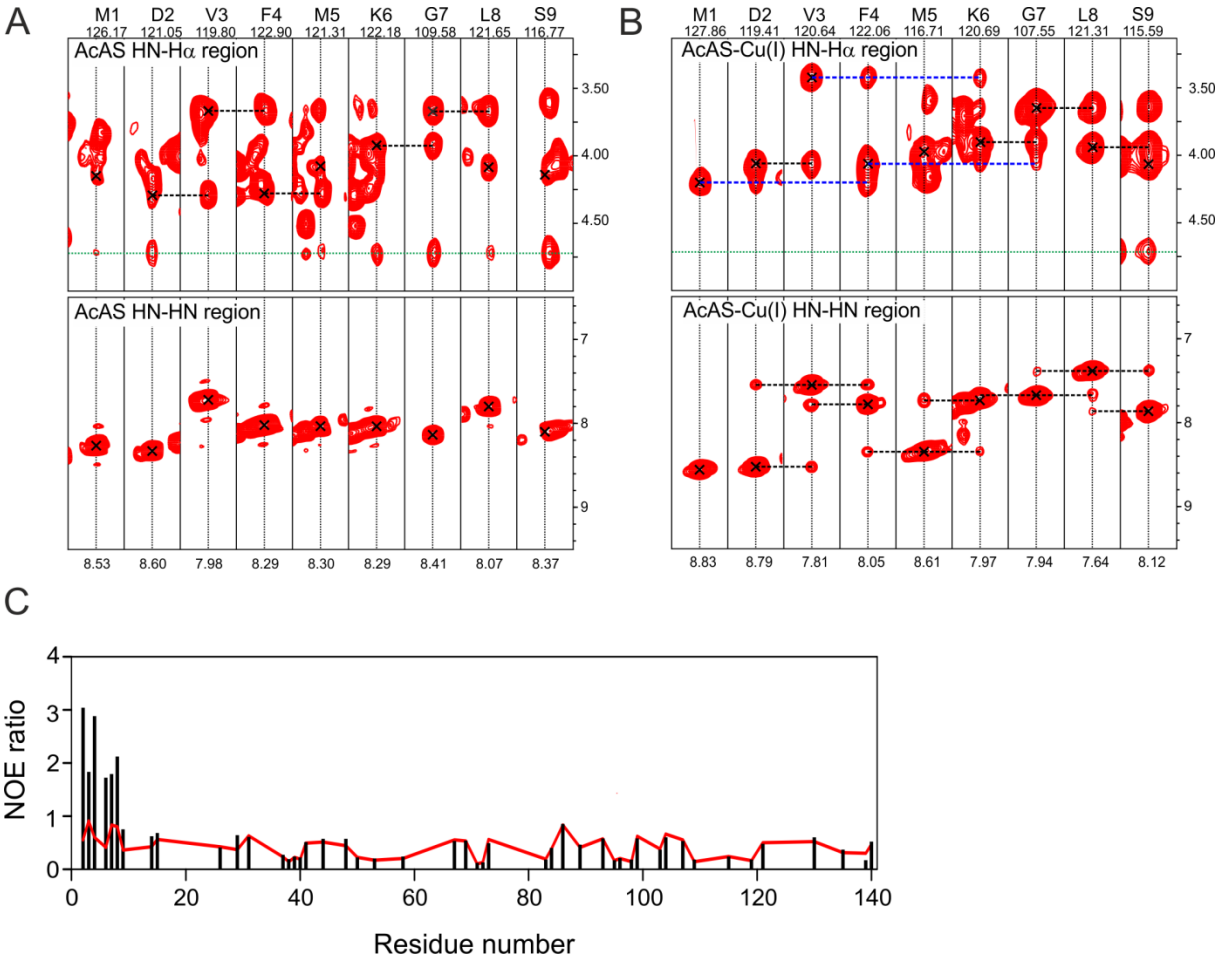

Supp. Fig. 5. ^{15}N-edited NOESY-HSQC strips corresponding to the N-α (top) and N-N (bottom) proton regions of the first 9 residues of AcAS in the absence (A) and presence (B) of 2 equiv. of Cu(I). Black crosses identify N-N diagonal proton correlations (bottom) and N-α intra-residue crosspeaks (top). Black dotted lines identify inter-residue $d_{NN}(i\text{-}1, i)$ and $d_{\alpha N}(i\text{-}1, i)$ NOE correlations. Blue dotted lines denote inter-residue $d_{H\alpha HN}(i\text{-}3, i)$ NOE peaks. The green dotted line identifies NOEs with water. (C) $d_{\alpha N}(i,i)/d_{\alpha N}(i\text{–}1,i)$ NOE intensity ratios measured for AcAS (red line) and AcAS-Cu(I) (black bars). Experiments were performed at 5°C using ^{15}N isotopically enriched AcAS samples (300 μM) dissolved in buffer A.

Supplementary Figure 6

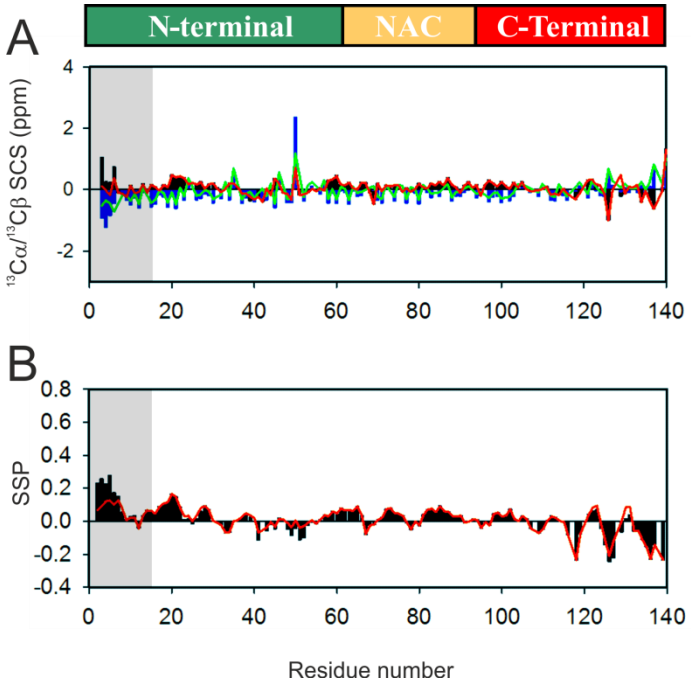

Supp. Fig. 6. Impact of Cu(I) binding on the structural properties of AS. (A) $^{13}C\alpha$ and $^{13}C\beta$ secondary chemical shifts measured for AS (red and green lines, respectively) and for its Cu(I)-bound form (black and blue bars, respectively). (B) Secondary structure propensity (SSP) of AS (red line) and its Cu(I)-bound form (black bars). Experiments were recorded at 15°C using AS (300 µM) samples dissolved in buffer A in the absence and presence of 5 equiv. of Cu(I).

Supplementary references

(1) Johnson, M.; Geeves, M. A.; Mulvihill, D. P. *Methods Mol. Biol.* **2013**, *981*, 193.

(2) Hoyer, W.; Cherny, D.; Subramaniam, V.; Jovin, T. M. *Biochemistry* **2004**, *43*, 16233.

(3) Schanda, P.; Kupce, E.; Brutscher, B. *J. Biomol. NMR* **2005**, *33*, 199.

(4) Bermel, W.; Bertini, I.; Felli, I. C.; Pierattelli, R. *J. Am. Chem. Soc.* **2009**, *131*, 15339.

(5) Farrow, N. A.; Zhang, O.; Forman-Kay, J. D.; Kay, L. E. *Biochemistry* **1997**, *36*, 2390.

(6) Zhang, H.; Neal, S.; Wishart, D. S. *J. Biomol. NMR* **2003**, *25*, 173.

(7) Marsh, J. A.; Singh, V. K.; Jia, Z.; Forman-Kay, J. D. *Protein Sci.* **2006**, *15*, 2795.

(8) Tamiola, K.; Mulder, F. A. *Biochem. Soc. Trans.* **2012**, *40*, 1014.

(9) Vuister, G. W.; Bax, A. *J. Am. Chem. Soc.* **1993**, *115*, 7772.

(10) Bertoncini, C. W.; Rasia, R. M.; Lamberto, G. R.; Binolfi, A.; Zweckstetter, M.; Griesinger, C.; Fernandez, C. O. *J. Mol. Biol.* **2007**, *372*, 708.

(11) Binolfi, A.; Fernandez, C. O.; Sica, M. P.; Delfino, J. M.; Santos, J. *Proteins* **2012**, *80*, 1448.

(12) Hill, R. B.; Flanagan, J. M.; Prestegard, J. H. *Biochemistry* **1995**, *34*, 5587.

(13) Serrano, L. *J. Mol. Biol.* **1995**, *254*, 322.

(14) Maltsev, A. S.; Ying, J. F.; Bax, A. *Biochemistry* **2012**, *51*, 5004.

(15) Cavanagh, J.; Fairbrother, W. J.; Palmer, A. G. I.; Rance, M.; Skelton, N. J. *Protein NMR Spectroscopy: Principles and Practice. Second Edition.* Elsevier Academic Press, California, U.S.A., 2007.

(16) Goddard, T. D.; Kneller, D. G. *Sparky 3*. San Francisco: University of California, 2002.

(17) Keller, R. L. J. *The Computer Aided Resonance Assignment Tutorial*. Cantina Verlag and Rochus Keller, Goldau, Switzerland, 2004.

(18) Binolfi, A.; Valiente-Gabioud, A. A.; Duran, R.; Zweckstetter, M.; Griesinger, C.; Fernandez, C. O. *J. Am. Chem. Soc.* **2011**, *133*, 194.

(19) Miotto, M. C.; Binolfi, A.; Zweckstetter, M.; Griesinger, C.; Fernandez, C. O. *J. Inorg. Biochem.* **2014**, *141*, 208.

(20) Miotto, M. C.; Rodriguez, E. E.; Valiente-Gabioud, A. A.; Torres-Monserrat, V.; Binolfi, A.; Quintanar, L.; Zweckstetter, M.; Griesinger, C.; Fernandez, C. O. *Inorg. Chem.* **2014**, *53*, 4350.

(21) Kuzmic, P. *Anal.Biochem.* **1996**, *237*, 260.

(22) Binolfi, A.; Quintanar, L.; Bertoncini, C. W.; Griesinger, C.; Fernandez, C. O. *Coord. Chem. Rev.* **2012**, *256*, 2188.

(23) Rasia, R. M.; Bertoncini, C. W.; Marsh, D.; Hoyer, W.; Cherny, D.; Zweckstetter, M.; Griesinger, C.; Jovin, T.; Fernández, C. O. *Proc. Natl. Acad. Sci. U. S. A.* **2005**, *102*, 4294.